Int. J. Heat Mass Transfer. Vol. 6, pp. 113–128. Pergamon Press 1963. Printed in Great Britain.

A FLAME ZONE MODEL FOR CHEMICAL REACTION IN A LAMINAR BOUNDARY LAYER WITH APPLICATION TO THE INJECTION OF HYDROGEN–OXYGEN MIXTURES*

PAUL A. LIBBY and CONSTANTINO ECONOMOS
Polytechnic Institute of Brooklyn, Aerodynamics Laboratory, Freeport, New York

(*Received* 14 *December* 1961 *and in revised form* 8 *June* 1962)

Abstract—There is suggested a model for chemical reaction within a boundary layer based on the concept of a critical temperature to distinguish between regions of frozen and equilibrium flow. The model, which is termed the flame zone model, is applied to the injection of hydrogen–oxygen mixtures through a porous surface into a laminar boundary layer with uniform external conditions in air. It is shown that the model is less restrictive than the frequently applied flame sheet model to which it reduces in special cases and with a simplifying approximation concerning the equilibrium condition. The results of several numerical examples corresponding to hypersonic wind tunnel and to hypersonic flight conditions are presented.

NOMENCLATURE

$A, B,$ constants in expression for temperature variation of K_p; see equation (41);
$a_1, a_2, b_1, b_2,$ constants in enthalpy–temperature relation; see equation (38) and Table 2;
$\bar{c}_p,$ specific heat of mixture;
$\bar{c}_{p_i},$ specific heat of ith species;
$c_f,$ skin friction coefficient based on free stream conditions;
$D_i,$ diffusion coefficient of ith species;
$f(\eta),$ Blasius function; see equation (1);
$g,$ total enthalpy ratio, h_s/h_{s_e};
$h,$ enthalpy of mixture;
$h_i,$ enthalpy of ith species;
$h_s,$ total enthalpy of mixture;
$k,$ thermal conductivity of mixture;
$K_p,$ equilibrium constant based on partial pressure;
$Le_i,$ Lewis number of ith species, $\rho D_i \sigma/\mu$;
$m,$ exponent in equation (5), $m = 0$ for planar flows, $m = 1$ for axisymmetric flow;
$M,$ Mach number;
$q,$ heat flux; see equations (30) and (31);
$r,$ radial distance from axis of symmetry;
$\tilde{s},$ transformed tangential co-ordinate; see equation (6);
$T,$ absolute temperature;
$T_r,$ reference temperature; see Table 2;
$T_f,$ ignition temperature; see Table 2;
$T_{\text{rec}},$ recombination temperature;
$T_{\text{dis}},$ dissociation temperature;
$u,$ tangential velocity component;
$U,$ non-dimensional velocity, $u/u_e \equiv f'$;
$v,$ normal velocity component;
$v_i,$ absolute velocity of ith species;
$V_i,$ diffusion velocity of ith species;
$W,$ molecular weight of mixture;
$W_i,$ molecular weight of ith species;
$\dot{w}_i,$ rate of production of ith species;
$x,$ tangential co-ordinate;
$y,$ normal co-ordinate;
$\tilde{Y}_i,$ mass fraction of ith element;

* This research was sponsored by the Aeronautical Research Laboratory, Office of Aerospace Research, United States Air Force, under Contract AF 33(616)-7661, Project 7064, and is partially supported by the Ballistic Systems Division.

Y_i, mass fraction of ith species;
Δ_i, enthalpy of ith species at $T = T_r$; see equation (36) and Table 2;
η, normal distance parameter; see equation (5);
μ, absolute viscosity of mixture;
ξ, injection parameter; see equation (27);
ρ, density of mixture;
ρ_i, partial density of ith species;
σ, Prandtl number, $\mu\bar{c}_p/k$;
τ_f, τ_c, characteristic flow and chemical times;
ϕ, parameter defining coolant composition; see equation (18).

Subscripts

c, conditions in coolant chamber;
e, conditions at edge of boundary layer;
f, conditions at edges of flame zone;
i, conditions corresponding to injection of inert gas;
o, conditions corresponding to zero injection;
w, conditions at wall or body surface.

INTRODUCTION

THERE has recently been an increasing interest in laminar boundary layers with chemical reaction as indicated by the appearance since 1958 of references [1–9] in the aeronautical literature. These studies have involved either simple chemical systems or limiting chemical behavior and simplified transport and thermodynamic properties. These simplifications are necessitated by the complexity of the boundary layer equations with realistic chemical, transport and thermodynamic descriptions. The simplification with respect to the chemical behavior is the most restrictive in that major features of practical interest are thereby obscured whereas assumptions with respect to transport and thermodynamic properties are expected to lead only to quantitative inaccuracies. Despite this limitation it is common to idealize chemical behavior in order to establish some features of boundary layers with chemical reaction. The actual applicability of these models depends on the model itself, the chemical system considered, and the flow conditions involved, e.g. the pressures, temperatures, velocities, and lengths.

The flame sheet model of chemical reaction has been considered by several authors (cf. references [3–9]). In this model chemical reaction is confined to one or more discontinuity surfaces which are located within the boundary layer by requirements on the composition and/or temperature at the sheet. Thus the flow is effectively frozen except at the flame sheets. This model has been used to predict the influence of chemical reaction on heat transfer and the location of reaction zones within a boundary layer.

It is the purpose of this report to suggest a model which is different from the flame sheet model but whose applicability in actual flows involves the same questions as does the flame sheet model. It is based on an idealization of chemical kinetic behavior in terms of a critical temperature T_f such that for $T < T_f$ no chemical reaction occurs while for $T > T_f$ equilibrium composition prevails.* It will be seen below that in general this idealization leads to reaction zones within the boundary layer rather than reaction surfaces and has therefore been termed a flame zone model.

As an example of its application consider the flow over a constant pressure, porous surface through which a fuel is injected into a stream involving an oxidizer. Assume that both T_w and T_e are less than T_f; assume further that chemical reaction occurs so that within the layer $T > T_f$.† Then there will exist a zone which is bounded on its two edges by surfaces corresponding to

* This idealization may be considered a combination of the ignition temperature concept employed in laminar flame theory plus an infinite reaction rate.

† As an extension of the utility of the suggested model, it could be assumed that if $T < T_f$ throughout the boundary layer in the case of completely frozen flow, then such a solution is a physically realistic one. However, if in that same flow, $T > T_f$ somewhere, then the assumption of a frozen flow is untenable. The only remaining, simple alternative is an equilibrium type of behavior possibly idealized as per the flame sheet or flame zone models. Non-equilibrium behavior is not considered a simple alternative although it is clearly the most realistic. There will be presented below a discussion of the role of pressure in determining the validity of equilibrium solutions for the hydrogen–oxygen–air system considered herein.

$T = T_f$ and which involves internally chemical equilibrium.

The details of the analysis and features of this model will be demonstrated by application to the injection of hydrogen and hydrogen–oxygen mixtures into a laminar boundary layer through a porous surface. Some attention has been devoted to the use of hydrogen as a coolant in porous cooling since it has long been recognized that the cooling effectiveness per unit weight of coolant is greatly increased if the molecular weight thereof is reduced. Thus Hartnett and Eckert [5] considered an incompressible boundary layer with hydrogen reaction and a flame sheet model for chemical reaction. Cohen *et al.* [3] considered, as one of several examples, hydrogen injection with a chemical model based on the specification of two temperatures: one for dissociation, T_{dis}, and one for recombination T_{rec} with $T_{\text{dis}} > T_{\text{rec}}$. For $T > T_{\text{dis}}$ water was assumed to vanish; for $T < T_{\text{rec}}$ either oxygen or hydrogen was assumed to vanish. Finally, Eckert *et al.* [10] and Hayday [7] considered hydrogen injection without chemical reaction.

It will be of interest to compare the boundary layer properties resulting from the proposed flame zone model for chemical reaction with those obtained from other chemical models and from hydrogen injection without reaction. It will be shown that the models are distinct; for example, the flame zone model is not limited in the injection rate and leanness of the oxygen–hydrogen mixtures used for cooling. In addition it displays a pressure dependence not found in the other model.

The detailed analysis of the flame zone model is discussed first in terms of the dependence of the gas properties within the layer on the velocity ratio $u/u_e \equiv U$; on the skin friction–mass transfer parameter, ξ; and on the ratio, ϕ, defining the composition of the hydrogen–oxygen mixture used as the coolant. The basic assumptions permitting this treatment are reviewed briefly. Then there are discussed heat transfer and boundary layer properties which result from application of the flame zone model to a laminar boundary layer. In a following section the results of numerical analysis for several free stream, wall and coolant conditions are presented and compared to the predictions of other models for chemical behavior.

ANALYSIS

The system considered corresponds to the injection through a porous surface of either hydrogen or a mixture of hydrogen and oxygen into a laminar boundary layer. The external flow is assumed to be uniform and to be air. The chemical species are taken to be oxygen, hydrogen, water in gaseous form and nitrogen. The subscripts 1–4 are employed respectively to denote these species. Note that nitrogen is treated here as an inert dilutant.*

Basic equations

For simplicity the distribution of injection and the transport properties will be assumed to be such that the flow is similar; thus

$$\text{(i)}\quad \sigma \equiv Le_i \equiv 1$$

$$\text{(ii)}\quad C \equiv (\rho\mu)/\rho_e\mu_e \equiv 1$$

$$\text{(iii)}\quad (\rho v)_w \sim x^{-1/2}.$$

With these assumptions the describing equations (cf. reference [2]) are

$$f''' + ff'' = 0 \tag{1}$$

$$g'' + fg' = 0 \tag{2}$$

$$\tilde{Y}_i'' + f\tilde{Y}_i' = 0, \quad i = 1, 2 \tag{3}$$

$$Y_4'' + fY_4' = 0 \tag{4}$$

where

$$(\,)' \equiv \mathrm{d}/\mathrm{d}\eta, \quad \eta \equiv \rho_e u_e r^m (2\tilde{s})^{-1/2} \int_0^y (\rho/\rho_e)\,\mathrm{d}y \tag{5}$$

$$\tilde{s} = \rho_e\mu_e u_e \int_0^x r^{2m}\,\mathrm{d}x \tag{6}$$

and where

$$\tilde{Y}_1 \equiv Y_1 + (W_1 Y_3/2W_3) \tag{7}$$

$$\tilde{Y}_2 \equiv Y_2 + (W_2 Y_3/W_3) \tag{8}$$

are the element mass fractions of oxygen and hydrogen respectively. Within the assumptions

* The analysis presented in the first several subsections of this section is a direct application to the hydrogen–oxygen–air system of previous analyses, e.g. those in references [2] and [6].

of similarity, these equations are independent of the chemical kinetics, i.e. they apply for frozen, non-equilibrium and equilibrium flows. The boundary conditions for these equations are:

$$\left.\begin{aligned} &\text{at } \eta = 0, && f = f_w, \quad f' = 0 \\ & && g = g_w \\ & && \tilde{Y}_i = \tilde{Y}_{iw}, \quad i = 1, 2 \\ & && Y_4 = Y_{4w}, \end{aligned}\right\} \quad (9)$$

$$\left.\begin{aligned} &\text{at } \eta \to \infty, && f' = g = 1 \\ & && \tilde{Y}_1 = Y_{1e} \\ & && \tilde{Y}_2 = 0 \\ & && Y_4 = Y_{4e}. \end{aligned}\right\} \quad (10)$$

The generalized Crocco relations

Comparison of the differential equations and boundary conditions leads to the generalized Crocco relations; namely

$$g = g_w(1 - f') + f' \quad (11)$$

$$\tilde{Y}_1 = \tilde{Y}_{1w}(1 - f') + Y_{1e}f' \quad (12)$$

$$\tilde{Y}_2 = \tilde{Y}_{2w}(1 - f') \quad (13)$$

$$Y_4 = Y_{4w}(1 - f') + Y_{4e}f'. \quad (14)$$

Use of the mass balance at the wall

The quantities $\tilde{Y}_{iw}$ and Y_{4w} are determined by requirements on the mass balance at the wall. It is first recognized that for steady flow there is no net flux of water and nitrogen into the wall; therefore,

$$v_{3w} = v_{4w} = 0 \quad (15)$$

and

$$(Y_1 v_1 + Y_2 v_2)_w = v_w. \quad (16)$$

Now conservation of mass between a plane in the coolant chamber where $\partial/\partial y \to 0$ and the exposed surface of the porous plate requires

$$\left.\begin{aligned} (\rho_1 v_1)_e &= (\rho_1 v_1)_w \\ (\rho_2 v_2)_e &= (\rho_2 v_2)_w \end{aligned}\right\} \quad (17)$$

and

$$(v_1)_e = (v_2)_e = v_e$$

so that if

$$(Y_1/Y_2)_e \equiv [(1 - Y_2)/Y_2]_e \equiv \phi, \quad (18)$$

then

$$(Y_1 v_1)_w = \phi(Y_2 v_2)_w. \quad (19)$$

Note that $\phi = W_1/2W_2 = 8$ corresponds to a stoichiometric mixture of hydrogen and oxygen in the coolant chamber.

It is now convenient to recognize that the diffusional velocities at the wall V_{iw} can be expressed as

$$V_{iw} = -[v_w/(-f_w)](Y'_i/Y_i)_w. \quad (20)$$

Use of (15), (16), (19) and (20) with $i = 1$ to 4 plus the relations

$$v_i = v + V_i \quad (21)$$

permits the following equations to be established:

$$Y'_{1w} = (-f_w)\{Y_{1w} - [\phi/(1 + \phi)]\} \quad (22)$$

$$Y'_{2w} = (-f_w)\{Y_{2w} - [1/(1 + \phi)]\} \quad (23)$$

$$Y'_{3w} = (-f_w)Y_{3w} \quad (24)$$

$$Y'_{4w} = (-f_w)Y_{4w}. \quad (25)$$

(7) and (12) are differentiated with respect to η and the results are evaluated at $\eta = 0$; then if (22) and (24) are employed to eliminate Y'_{iw}, $i = 1, 3$, there results

$$\tilde{Y}_{1w} = \{Y_{1e} + [\phi\xi/(1 + \phi)]\}(1 + \xi)^{-1} \quad (26)$$

where

$$\xi \equiv (-f_w)/f''_w \equiv 2(\rho v)_w/\rho_e u_e c_f. \quad (27)$$

Similarly,

$$\tilde{Y}_{2w} = [\xi/(1 + \phi)](1 + \xi)^{-1}. \quad (28)$$

Also (14) is differentiated with respect to η; the result is evaluated at $\eta = 0$ and combined with (25) to yield

$$Y_{4w} = Y_{4e}(1 + \xi)^{-1}. \quad (29)$$

Thus (26), (28) and (29) combined with (12)–(14) permit the element mass fractions to be expressed in terms of f', ϕ and ξ once Y_{1e} and

Y_{4e} are specified. However, the corresponding composition in terms of the mass fractions Y_i is still undetermined in terms of these same parameters.

It will be convenient for further analysis to have the values f''_w for various values of $-f_w$. These can be obtained from the tabulation of Emmons and Leigh [11]; the results in terms of the variables employed herein are shown in Fig. 1.

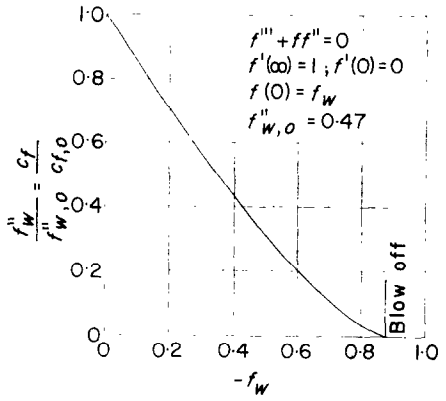

FIG. 1. Ratio of friction coefficient with injection to that on solid wall as function of injection rate.

Heat transfer at the wall

It is of interest to consider the heat transfer at the wall to ascertain what can be determined prior to specification of the model for the chemical reaction. Define the heat transfer

$$q \equiv [\mu(h_s)_y]_w = [(\rho v)_w h_{s_e}/(-f_w)]g'_w. \quad (30)$$

Now from (11) and (27) it is easily seen that

$$q = \rho_e u_e h_{s_e}(c_f/2)(1 - g_w). \quad (31)$$

Furthermore, the skin-friction coefficient c_f is a function of Reynolds number and of $(-f_w)$; thus, if there can be made some auxiliary statement leading to the determination of g_w, then q can be found independent of the chemical model. Such statements can be, for example, either $|g_w| \ll 1$ or $Y_{1w} \simeq 0$. This result is a special case of the more general results which concern heat transfer when the Lewis number is unity and which were developed by Lees [6].

It may also be noted here that the considerations presented thus far suffice to determine the heat transfer if it is assumed that no chemical reaction occurs. In this case $\tilde{Y}_1 \equiv Y_1$, $\tilde{Y}_2 \equiv Y_2$ and $Y_3 \equiv 0$. Hence (26), (28) and (29) completely define the composition at the wall and permit the determination of q for given wall temperature and flow conditions. Evidently

$$q/q_i = (1 - g_w)/(1 - g_{wi}) \quad (32)$$

where the subscript i corresponds to the case of no chemical reaction; (32) is utilized later in the presentation of some of the numerical results. Note that $q < q_i$, if $g_w < g_{wi} < 1$, i.e. chemical reaction leads to reduction in heat transfer provided this inequality is satisfied.

Energy balance

If the porous surface is assumed to be cooled only by an increase in the enthalpy of the coolant, then an energy balance yields

$$(\sum_{i=1}^{2} \rho_i v_i h_i)_e - (\sum_{i=1}^{4} \rho_i v_i h_i)_w + \left(k \frac{\partial T}{\partial y}\right)_w = 0. \quad (33)$$

(15)–(21) and (30) permit (33) to be written as

$$(\rho v)_w(h_e - h_w) + q = 0. \quad (34)$$

Now (31) can be employed to determine g_w as

$$g_w = (\xi g_e + 1)(1 + \xi)^{-1}. \quad (35)$$

It is of interest to note that (35) provides another auxiliary statement concerning g_w which can be employed in (31) to yield q independent of the chemical behavior.

Approximate relation for the static temperature

It will be convenient to employ approximations to the static enthalpy–temperature relation for the species. For most purposes it is sufficiently accurate to let

$$h_i = \Delta_i + \bar{c}_{p_i}(T - T_r) \quad (36)$$

where Δ_i is the enthalpy of species i at the temperature T_r and $\bar{c}_{p_i}$ is an appropriate average value of the specific heat of species i. Then (11) and (36) yield

$$T = T_r + \{[g_w(1 - f') + f']h_{s_e} - \sum_{i=1}^{4} Y_i\Delta_i - (u_e^2/2)f'^2\}(\sum_{i=1}^{4} Y_i\bar{c}_{p_i})^{-1}. \quad (37)$$

Note that additional flow parameters, g_w, h_{s_e} and $u_e^2/2$, arise from the energy equation and further that g_w must be computed as part of the solution as discussed in connection with the heat transfer.

Flame zone model—general considerations

Consider next the determination of the state within the boundary layer, and the heat transfer when g_w is unknown and significant. A model for the chemical behavior is required to supplement the previously described system of equations for the element mass fractions. Note that knowledge of one species mass fraction, either Y_1, or Y_2 or Y_3, completes specification of the state of the gas since aside from nitrogen there are three species and two element mass fractions. In the subsequent analysis, Y_1 will arbitrarily be selected as the species mass fraction to be determined. It is therefore convenient to express the temperature as

$$T = T_r + \{[g_w(1 - f') + f']h_{s_e} - [b_1 Y_1 + b_2 \tilde{Y}_1 + \Delta_2 \tilde{Y}_2 + \Delta_4 Y_4] - (u_e^2/2)f'^2\} \{a_1 Y_1 + a_2 \tilde{Y}_1 + c_{p_2} \tilde{Y}_2 + c_{p_4} Y_4\}^{-1} \quad (38)$$

where

$$a_1 = c_{p_1} + (2W_2 c_{p_2} - 2W_3 c_{p_3})/W_1$$

$$a_2 = c_{p_1} - a_1$$

$$b_1 = \Delta_1 + (2W_2 \Delta_2 - 2W_3 \Delta_3)/W_1$$

$$b_2 = \Delta_1 - b_1$$

and the mixture molecular weight as

$$W^{-1} = [\sum_{i=1}^{4} (Y_i/W_i)] = (Y_1/W_1) + (\tilde{Y}_2/W_2) + (Y_4/W_4). \quad (39)$$

There will be now discussed in detail the flame zone model; accordingly, it is assumed that there exists a critical temperature T_f below which no chemical reaction takes place and above which the flow is in equilibrium. The actual selection of T_f is somewhat arbitrary but can be considered in terms of the flow and chemical times characterizing the system and denoted by τ_f and τ_c respectively. For example, ignition delay times in the hydrogen–oxygen–air system under consideration (cf. reference [12]) can be employed as a measure of the chemical time and T_f selected so that $\tau_c \ll \tau_f$. For this chemical system it should be noted that the pressure is important in determining the validity of the ignition delay time as a measure of the chemical time. It is known from the results of references [13] and [14] that the decay of intermediates such as the atomic oxygen and atomic hydrogen, created during the period defined by the ignition delay, leads to the chemical energy release associated with the hydrogen–oxygen reaction. This decay corresponds to a third order, recombination process and is therefore pressure sensitive. Roughly, the ratio of the overall reaction time to the ignition delay is inversely proportional to the pressure, being about 10 for a pressure of 1 atm. Accordingly, equilibrium models of chemical behavior for the chemical system under discussion will be realistic only for pressure on the order of several atmospheres or more and for temperatures in frozen flow sufficiently high so that the ignition delay time is small compared to the characteristic flow time.

The application of the flame zone model to the determination of boundary-layer characteristics results in the division of the domain of the velocity ratio, f', into sections wherein $w_i \equiv 0$ and other sections wherein chemical equilibrium prevails. In the latter sections, the element mass fractions, the mass fraction of nitrogen, and one other species mass fraction, e.g. Y_1, can be related according to the following equations:

$$K_p^2 = (pW)^{-1}(W_2^2 W_1/W_3^2)(Y_3^2/Y_2^2 Y_1) \quad (40)$$

$$= \{(4/pW)(W_2^2/W_1)(\tilde{Y}_1 - Y_1)^2\} \{Y_1[\tilde{Y}_2 - (2W_2/W_1)(\tilde{Y}_1 - Y_1)]^2\}^{-1}. \quad (40a)$$

The equilibrium constant K_p is a known function of the temperature;* for numerical convenience it can be approximated as

$$K_p \simeq Be^{A/T}. \quad (40b)$$

For example, in the temperature range $500 < T < 2000°K$, with

* K_p is denoted $K_{p,4}$ in reference [15] and is tabulated therein.

$$A = 29{\cdot}950°\text{K}$$

$$B = 1{\cdot}1138(10^{-3})\ \text{atm}^{-1/2} \qquad (41)$$

the exact function $K_p = K_p(T)$ is approximated within a few per cent. It should be noted that for $T \lesssim 2000°\text{K}$, $K_p \gg 1$ so that in equilibrium states either Y_2 or Y_1 or both are small compared to unity. (37), (39), (40a) and (40b) permit the state of the gas within the equilibrium sections of the domain of the velocity ratio to be determined since as discussed previously the element mass fractions $\tilde{Y}_i i = 1, 2$ are known in terms of f', ϕ and ξ.

The boundaries of the domains are determined by the following considerations: assume that ϕ, ξ are given; let $f' = (f')_f \equiv U_f$ denote the velocity ratio at an edge of a flame zone. At such an edge $T = T_f$ and equilibrium prevails; thus (37), (39), (40a) and (40b) with $T = T_f$ and the equations yielding $\tilde{Y}_i$, $i = 1, 2$ and Y_4 in terms of f', define Y_{1f} and U_f provided g_w is determined; clearly, an additional relation is still required for the determination of Y_{1f}, U_f and g_w. Note that g_w can be expressed in terms of T_w, $\tilde{Y}_i$, $i = 1, 2$, Y_4 and Y_1; there results

$$g_w = h_{s_e}^{-1}[(T_w - T_r)(\Sigma c_{p_i} Y_i)_w + (\Sigma Y_i \Delta_i)_w] \qquad (42)$$

$$= h_{s_e}^{-1}\{\Delta T_w[a_1 Y_{1w} + a_2 \tilde{Y}_{1w} + c_{p_2}\tilde{Y}_{2w} + c_{p_4} Y_{4w}] + b_1 Y_{1w} + b_2 \tilde{Y}_{1w} + \Delta_2 \tilde{Y}_{2w} + \Delta_4 Y_{4w}\}$$

where

$$\Delta T_w = T_w - T_r.$$

Case (a): $T_e, T_w < T_f$

It is most convenient in discussing the further details of the flame zone model, i.e. the determination of Y_{1f}, U_f, and g_w, to consider the several cases which are characterized by the wall and external temperatures. Shown in Figs. 2a–c are three such cases;* the first (Fig. 2a) corresponds to T_e, $T_w < T_f$. There then arise two zones wherein $\dot{w}_i \equiv 0$, one close to the wall and the other near the outer edge. Denote the velocity ratio at the inner edge of the reaction

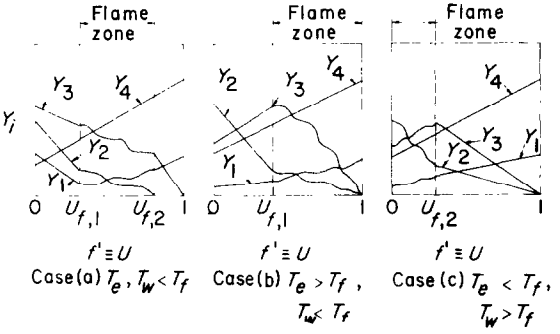

FIG. 2. Schematic representation of composition distributions.

zone as $U_{f,1}$ and that at the outer edge as $U_{f,2}$. In the inner region the Crocco relation holds for Y_1 so that

$$Y_1 = Y_{1w} + (Y_{1f,1} - Y_{1w})[f'/U_{f,1}], \qquad 0 \leqslant f' \leqslant U_{f,1} \qquad (43)$$

where $U_{f,1}$, Y_{1w} and $Y_{1f,1}$ are unknown. The additional equation required to define the inner layer is found as follows; solve for Y_{1w} from (22) and (43) by differentiating (43) with respect to η and by eliminating the derivative $(Y_1')_w$ in (22); there results

$$Y_{1w} = [(\phi\xi U_{f,1})/(1 + \phi) + Y_{1f,1} + (1 + U_{f,1}\xi)^{-1}. \qquad (44)$$

Now (43), with Y_{1w} eliminated by substitution of (44) provides the requisite equation relating $Y_{1f,1}$, $U_{f,1}$ and g_w. The set of equations defining the location of the flame zone are non-linear and algebraic-transcendental. An iterative method of solution can be employed.† Note that if only the heat transfer is of interest, the calculation is completed by the determination of g_w.

The determination of $U_{f,2}$ is straightforward since g_w has been determined from the solution of the inner region. The distribution of Y_1 in the outer region is given again by the Crocco relation for Y_1 in the form

$$Y_1 = [Y_{1e}(f' - U_{f,2}) + Y_{1f,2}(1 - f')](1 - U_{f,2})^{-1}, \quad U_{f,2} \leqslant f' \leqslant 1 \qquad (45)$$

* Note that a fourth case T_w, $T_e > T_f$ is trivial with respect to the chemical model under consideration since it corresponds to equilibrium chemical behavior throughout the boundary layer.

† The calculations are similar to the usual equilibrium calculations with auxiliary conditions, as for example, those involved in detonation waves satisfying the Chapman–Jouget condition (cf. reference [15]).

where $Y_{1f,2}$ is determined by equilibrium considerations at the outer edge of the reaction zone.

Case (b): $T_e > T_f$, $T_w < T_f$

For this case there is one zone of frozen flow close to the surface as shown in Fig. 2(b). The analysis applicable to the inner layer of the above case applies here so that the edge of the reaction zone occurs at a velocity ratio U_f denoted in the previous case as $U_{f,1}$. Note that specification of equilibrium composition at the outer edge, i.e. as $f' \to 1$ results in an indeterminancy ($\tilde{Y}_1 \to Y_1 \to Y_{1e}$, $\tilde{Y}_2 \to 0$) permitting K_p to take on the value corresponding to $T = T_e$.

Case (c): $T_w > T_f$, $T_e < T_f$

As shown in Fig. 2(c) this case involves a reaction zone adjacent to the wall. The wall enthalpy ratio given in this case can be obtained by applying the equilibrium condition, (40a) with $T = T_w$, $\tilde{Y}_i = \tilde{Y}_{iw}$, $i = 1, 2$, and $Y_4 = Y_{4w}$, in order to determine Y_{1w} and by subsequently evaluating g_w from (42). As in Cases (a) and (b) the velocity ratio at the edge of the reaction zone, denoted again by U_f, can be obtained from the equilibrium conditions. In the outer portion of the domain of the velocity ratio the mass fraction Y_1 satisfies a Crocco relation of the form given by (44) with $U_{f,2}$ replaced by U_f.

Relation to flame sheet model and a simplifying approximation

In some cases the analysis of the flame zone model discussed above is simplified by the aforementioned observation that for values of T_f on the order of 1000°K, the equilibrium constant is large, implying Y_1 or Y_2 or both small. Thus in some cases it is possible to let either $Y_{1f} \simeq 0$ or $Y_{2f} \simeq 0$ and thereby to obtain simply an approximate solution for the composition in terms of the velocity ratio f'. Furthermore, this approximation effectively reduces the flame zone model to the flame sheet model under certain circumstances. The fact that this reduction is not generally possible implies an essential difference between the two models of chemical behavior.

As an example of the approximation consider a case corresponding to Fig. 2(a) with the injected gas a rich mixture of hydrogen and oxygen ($\phi \leqslant 8$). Now at the inner edge of the reaction zone it would be expected on physical grounds that $Y_{1f,1} \simeq 0$. Then (37) with $T = T_f$, (42) and (44) with $Y_{1f,1} = 0$ are three equations yielding $U_{f,1}$, g_w and Y_{1w}. At the outer edge of the reaction zone it would be expected that $Y_{2f,2} \simeq 0$ and thus from (7) and (8) that

$$[\tilde{Y}_2 - (2W_2/W_1)(\tilde{Y}_1 - Y_1)]_{f,2} \simeq 0. \quad (46)$$

(46) along with (12), (13), (26) and (28) and (37) with $T = T_f$ and with g_w determined from the calculation of the inner edge are two equations giving $U_{f,2}$ and $Y_{1f,2}$. In this case the approximation to the equilibrium condition only simplifies the analysis without altering the character of the composition distributions in terms of f'. However, if in Case (a) $\phi \geqslant 8$, i.e. a lean mixture of hydrogen and oxygen is injected, then equilibrium at the inner edge of the reaction zone implies $Y_{2f,1} \simeq 0$; but then the reaction zone effectively vanishes and the flame zone reduces to a sheet. Moreover, Case (b) with $\phi \geqslant 8$ by the same reasoning reduces to a flame sheet and is thus identical with Case (a) for the same values of ϕ. Finally in Case (c) with $\phi \geqslant 8$, $Y_{2,f} \simeq 0$ although a zone of reaction would prevail.*

It should be noted that the approximation relative to the mass fractions at the edge of the flame zone precludes consideration of rates of injection so low that oxygen from the free stream diffuses to the wall. The critical values of ξ corresponding to the lowest value of the injection may be determined as follows: elimination of Y_3 between (7) and (8) yields

$$Y_2 = \tilde{Y}_2 - (2W_2/W_1)(\tilde{Y}_1 - Y_1). \quad (47)$$

Hence, for $Y_{1f,1} \approx 0$

$$Y_{2f,1} = \tilde{Y}_{2f,1} - (2W_2/W_1)\tilde{Y}_{1f,1}. \quad (48)$$

Utilizing (12) and (13) gives

$$Y_{2f,1} = (1 - U_{f,1})[\tilde{Y}_{2w} - (2W_2/W_1)\tilde{Y}_{1w}] - (2W_2/W_1)U_{f,1}Y_{1e}. \quad (49)$$

Evidently, to fulfill the physical requirement that $Y_{2f,1} \geqslant 0$ it follows from (49) that the inequality

$$\tilde{Y}_{2w} - (2W_2/W_1)\tilde{Y}_{1w} \geqslant 0 \quad (50)$$

* Note that from the point of view taken here there si no difficulty associated with $\phi > 8$. The flame sheet model fails for this case (cf. reference [8]).

must be satisfied. Using (26) and (28) in (50) leads to the requirement

$$[(8 - \phi)/(1 + \phi)]\xi \geqslant Y_{1e}$$

so that the range of values of ξ for which the assumption $Y_{1f,1} \simeq 0$ holds is

$$\xi \geqslant \left(\frac{1 + \phi}{8 - \phi}\right) Y_{1e}. \qquad (51)$$

It is further required that $\phi < 8$. It is interesting to note that these inequalities are precisely the conditions which must be satisfied for physically meaningful solutions according to the flame sheet analysis as discussed by Eschenroeder [8]. However, the flame zone model applied without the aforementioned approximation $Y_{1,f} \simeq 0$ provides continuous behavior as $\xi \to 0$.

Finally, it should be noted that the approximation being discussed effectively eliminates the pressure from the determination of the location of the flame zone. The pressure would, however, influence the composition within the flame zone in the region where both the oxygen and hydrogen are present in small amounts. Of course, the previous discussion regarding the role of the pressure in determining the validity of the model for the hydrogen–oxygen–air system must not be overlooked. Note that there is no pressure dependence in the flame sheet model.

NUMERICAL EXAMPLES

To indicate some of the features of the flame zone model discussed above and to compare its predictions with other models of chemical behavior, several numerical examples have been carried out. These have involved several sets of external flow conditions, two corresponding to conditions in a typical hypersonic wind tunnel and the others to typical conditions in hypersonic flight. The flow and wall conditions assumed are listed in Table 1; the values of the thermodynamic parameters employed are given in Table 2. The pressure was arbitrarily taken to be 1 atm although somewhat higher pressures may be required for the validity of the model. At 1 atm a temperature of 1100°K leads to an ignition delay on the order of 10 μ and an overall reaction time of 300 μ. Thus for flow times on the order of several milliseconds, an ignition temperature of 1100°K is reasonable and has been used for the numerical analysis herein. The wall external stream temperatures have been chosen so that the various cases shown in Fig. 2 occur.

Table 1. Flow parameters used in the numerical calculations

	M_e (approx)	h_{s_e} (cal/gm)	T_e (degK)	T_w (degK)	p_e (atm)
Hypersonic flight conditions	10·2 11·8	4444	1300 900	1200 900 600	1
Wind tunnel conditions	2·4 3·8	750	1300 900	1200 900 600	1

Table 2. Thermodynamic parameters used in the numerical calculations

Parameter	
T_r	2000°K
T_f	1100°K
$\bar{c}_{p_1}$	0·283 cal/g degK
$\bar{c}_{p_2}$	4·10 cal/g degK
$\bar{c}_{p_3}$	0·656 cal/g degK
$\bar{c}_{p_4}$	0·303 cal/g degK
Δ_1	442 cal/g
Δ_2	6324 cal/g
Δ_3	−2250 cal/g
Δ_4	479 cal/g
a_1	0·05854 cal/g degK
a_2	0·2249 cal/g degK
b_1	3766 cal/g
b_2	−3324 cal/g

The calculations include the determination of the heat transfer rates at the porous surface, as well as the concentration and temperature profiles within the boundary layer. The numerical analysis was carried out on the Bendix G-15 computer at the PIBAL and as mentioned previously, involved at most the solution of simultaneous algebraic equations. For all except the lowest values of ξ the approximation relative to the vanishing of either oxygen or hydrogen at the edges of the flame zone was employed. For the region of chemical equilibrium a trial and error procedure to obtain solutions was used for the determination of the composition and temperature. Except in regions where both the hydrogen and oxygen were present in small

amounts, the procedure converged rapidly; in these particular regions special care had to be exercised to assure convergence.

Results of heat transfer

The heat-transfer data are presented in Figs. 3–8. In the calculations presented in these figures the influence of the external temperature T_e was found to be negligible; therefore the results are applicable to all values of T_e employed herein. In Figs. 3 and 4 the variation of the heat flux rate q with $-f_w$ is compared to that occurring on an impermeable wall under identical flow conditions. This ratio, denoted by q/q_o, may be obtained from (31) and the definition of q_o. There results

$$\frac{q}{q_o} = \frac{c_f}{c_{f_o}} \frac{1 - g_w}{1 - g_{w,o}} \tag{52}$$

where c_{f_o} and $g_{w,o}$ denote the skin friction coefficient and total enthalpy ratio at a solid wall (zero injection). For a given wall temperature, $g_{w,o}$ is easily computed, i.e. from (42) with $Y_{1w} = Y_{1e}$, and c_f/c_{f_o} is a known function of $-f_w$ (cf. Fig. 1). Hence, calculation of g_w yields the corresponding value of q/q_o.

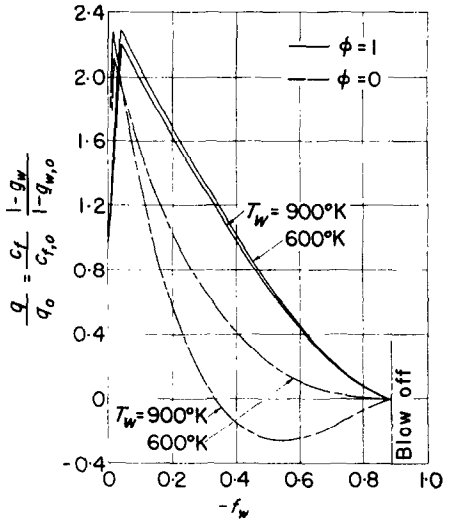

FIG. 3. Variation of heat-transfer ratio q/q_o with injection parameter f_w, wall temperature T_w, and coolant composition ϕ—wind tunnel conditions.

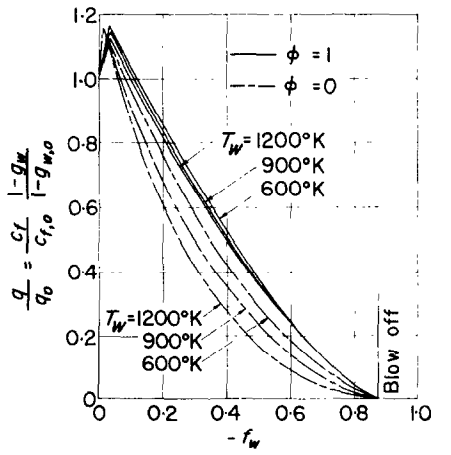

FIG. 4. Variation of heat-transfer ratio q/q_o with injection parameter f_w, wall temperature T_w, and coolant composition ϕ—flight conditions.

The results in Figs. 3 and 4 indicate that cooling of the surface may be achieved in all cases for sufficiently high rates of injection. Thus the increase in the heat fluxes associated with combustion and with the resultant formation of water within the boundary layer is more than balanced by the reduction due to the mass transfer. For low rates of injection under wind tunnel conditions, heat transfer considerably greater than that associated with an impermeable surface can occur. The effectiveness of the coolant is decreased significantly by the injection of hydrogen–oxygen mixtures rather than pure hydrogen. This result is primarily a consequence of the relatively high molecular weight of the oxygen–hydrogen mixture, although the increase in the production of water and the correspondingly higher energy release also contribute to the degradation of cooling effectiveness. The dependence of the heat transfer on wall temperature is greatly reduced by both an increase in free stream Mach number as shown by Lees [6] and others and by the addition of oxygen to the coolant.

The existence of negative values of q/q_o shown in Fig. 3 is of interest and is due to the low energy of the external flow corresponding to wind tunnel conditions. The conductive heat transfer in the range of ξ giving $q/q_o < 0$ is positive but is dominated by negative energy transfer due to diffusion of hydrogen from the wall. The values of g_w, again in this range of ξ, are greater than unity for sufficiently high wall

temperatures. Injection of even a small amount of oxygen with the coolant ($\phi \simeq 1$) causes an increase in the heating potential to which the wall is exposed; the wall enthalpy is reduced considerably and, in fact, can become negative. This behavior is illustrated by the marked shift of the curve of q/q_o from the negative region for $\phi = 0$, to positive values for $\phi = 1$. Under hypersonic flight conditions this behavior does not appear (cf. Fig. 4) since, for high Mach numbers (and hence high values of h_{se}), g_w is always less than unity.

As mentioned previously at the low rates of injection the assumption that Y_1 vanishes at the inner edge of the flame zone becomes progressively less tenable. In particular, for ξ equal to the value defined by (51) or less, the assumption is not valid and must be replaced by the exact condition of equilibrium at the edges of the flame zone. The calculations then yield the results shown in Figs. 3 and 4 in the neighborhood of $\xi = 0$; the ratio $q/q_o \to 1$, and the concentration profiles approach the uniform distribution $Y_1 \equiv Y_{1e}$, $Y_4 \equiv Y_{4e}$, $Y_2 = Y_3 = 0$. The values of q/q_o as obtained by either the exact equilibrium considerations or by using the approximation $Y_{1f,1} = 0$ are numerically identical when computed for the injection parameter equal to the limiting value defined by (51).

In Fig. 5 the heat-transfer results are compared with that corresponding to the injection of inert gas with the same molecular weight.

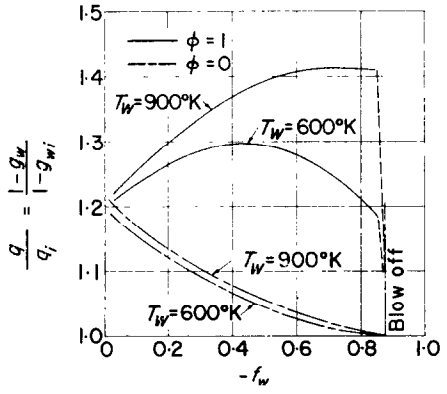

FIG. 5. Ratio of heat transfers to wall with and without combustion (q/q_i) as a function of injection parameter f_w and coolant composition ϕ—flight conditions

As may be expected the cooling effect is diminished in all cases by the chemical reaction.

Fig. 6 shows a comparison of the results obtained for one case, using the present flame zone model with that obtained with a flame sheet model, as by Eschenroeder [8]. As can be seen therein, the flame zone model predicts somewhat higher values of the heat transfer for injection rates of practical interest although the predictions of the two models are in close agreement.

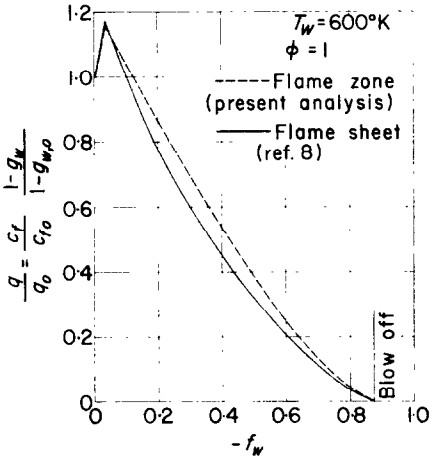

FIG. 6. Comparison of predictions of the flame sheet and flame zone models for heat-transfer ratio (q/q_o)—flight conditions.

Coolant temperatures for an energy balance

In Figs. 7 and 8 are shown the values of coolant temperature T_c required in order to maintain in the exposed surface at a prescribed temperature, T_w, with a given injection rate. This value of T_c is determined by solving for g_c from (35). Then T_c can be evaluated for a particular coolant composition (i.e. prescribed value of ϕ). The points at which the curves intersect the abscissa in Figs. 7 and 8 correspond to the minimum values of the injection rate necessary to maintain the assigned wall temperature T_w. (Evidently this minimum cannot be realized in practice since the coolant gases would have to be at absolute zero temperature.) As can be seen from these figures, the addition of even a small amount of oxygen to the mixture greatly increases the rate at which the coolant must be injected. This is further confirmation of

the effectiveness of pure hydrogen as a coolant. Furthermore, it can be shown that regardless of the value of ϕ, if the coolant rate corresponds to blowoff, the required value of T_c approaches T_w.* This is indicated by the broken lines joining the ends of the solid curves to the points $T_c = T_w$ at the blowoff value of $-f_w$. It was not possible to perform the actual computations in this limiting region because of the singular behavior of the parameter ξ which appears explicitly in the analysis.

Temperature profiles

The effects of injection rate, of coolant composition, and of external and wall temperatures on the temperature distributions in the boundary layer in terms of η are shown in Figs. 9–13. The calculations of these profiles have been

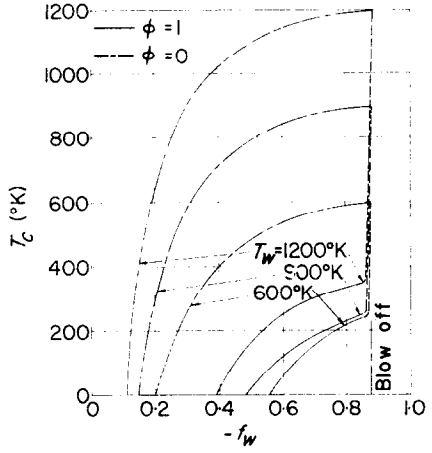

FIG. 7. Variation of coolant temperature T_c with injection parameter f_w and coolant composition ϕ—wind tunnel conditions.

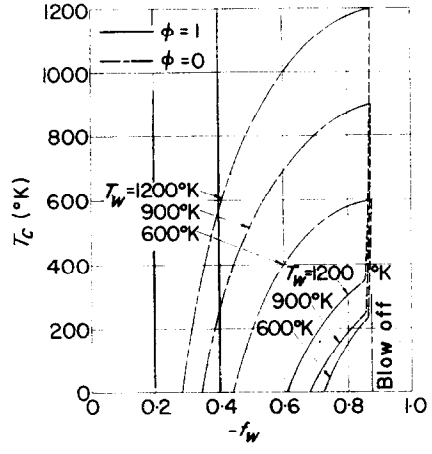

FIG. 8. Variation of coolant temperature T_c with injection parameter f_w and coolant composition ϕ—flight conditions.

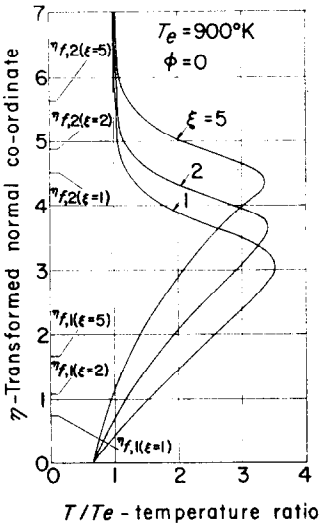

FIG. 9. Effect of injection parameter ξ on temperature profile—Case (a).

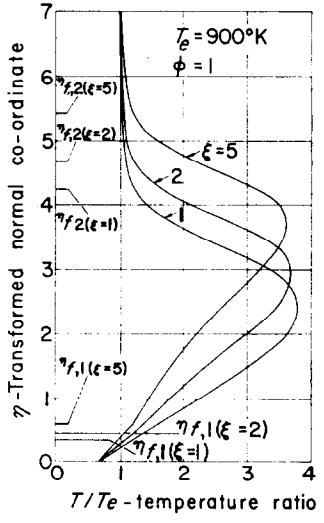

FIG. 10. Effect of injection parameter ξ on temperature profile—Case (a).

* The details of the proof thereof are given in Appendix A.

carried out only for the case of flight conditions involving combinations of external and wall temperatures shown in Fig. 2.

These figures indicate the following; the maximum temperature is not greatly affected by the rate of injection, by the injection of a small amount of oxygen along with the hydrogen ($\phi = 1$), or by the external and wall temperatures. The value of η at the point of maximum

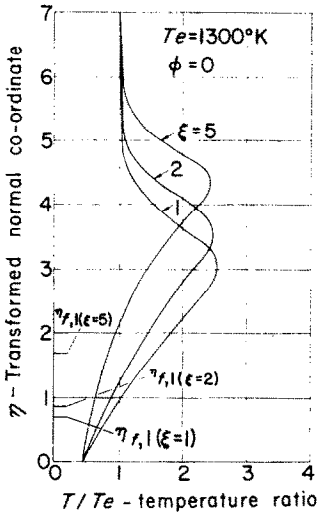

FIG. 11. Effect of injection parameter ξ on temperature profile—Case (b).

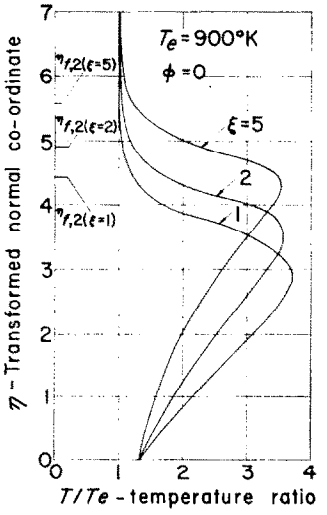

FIG. 12. Effect of injection parameter ξ on temperature profile—Case (c).

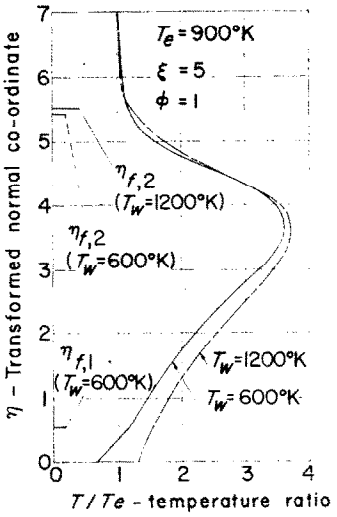

FIG. 13. Effect of wall temperature T_w on temperature profile—flight conditions.

temperature is increased by an increase in the rate of injection.* The inner edge of the flame zone in Case (a) and the edge in Cases (b) and (c) move further from the wall as the rate of injection increases. In Case (a) the inclusion of oxygen in the coolant moves the edge of the flame zone closer to the wall.

Concentration profiles

In Figs. 14–16 there are presented the concentration profiles for flight conditions and for various rates of injection and various wall temperatures. From these figures the following will be noted: for Case (a) with $\phi = 1$, the concentrations of oxygen and hydrogen at the surface increase with the rate of injection while the concentration of nitrogen decreases and that of water remains unchanged. In this same case there exists within the flame zone a region with negligible oxygen present; thus there are two separate regions with oxygen present. In Case (c), on the contrary, the concentrations of water and nitrogen at the surface decrease with increasing rates of injection and oxygen appears only near the outer edge of the flame zone. When the wall temperature is increased above the

* In the physical (x,y) plane these points would tend to be closer.

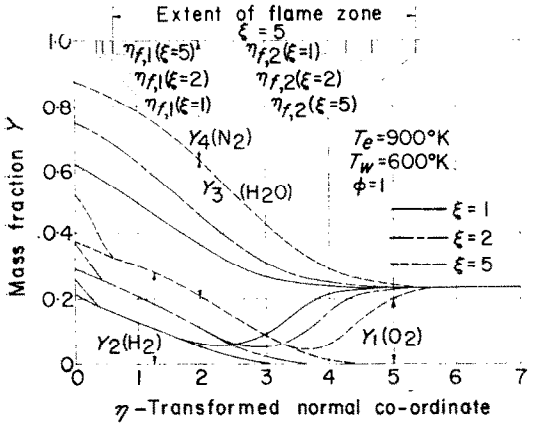

FIG. 14. Effect of injection parameter ξ on concentration profiles—Case (a)—flight conditions.

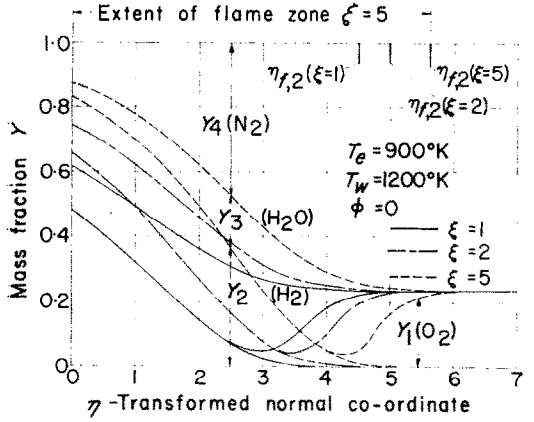

FIG. 15. Effect of injection parameter ξ on concentration profiles—Case (c)—flight conditions.

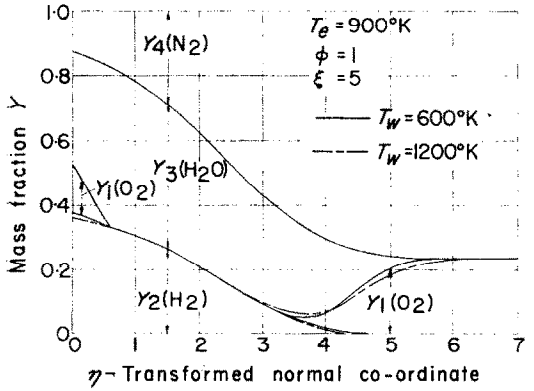

FIG. 16. Effect of wall temperature T_w on concentration profiles—flight conditions.

critical temperature, T_f, the oxygen at the surface effectively vanishes even if oxygen is injected in the coolant.

Comparison of profiles with other models

In Figs. 17 and 18 a comparison of the temperature and concentration profiles as predicted by the flame sheet and flame zone models for combustion is presented. This comparison reveals that the two models differ significantly in the prediction of the detailed structure of the boundary layer. The difference in the wall

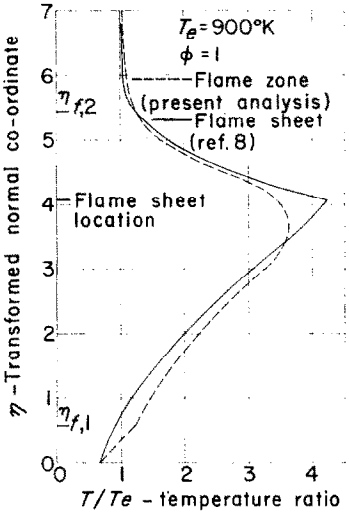

FIG. 17. Comparison of predictions of the flame sheet and flame zone models for the temperature profile—Case (a).

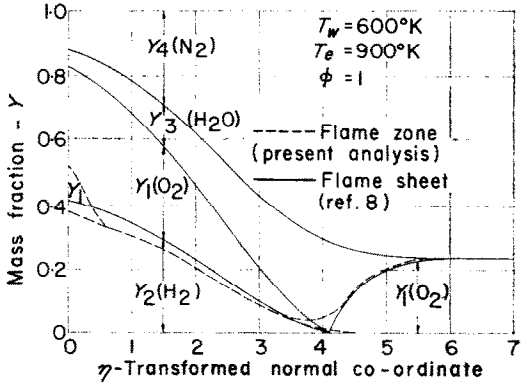

FIG. 18. Comparison of predictions of the flame sheet and flame zone models for the concentration profiles—Case (a).

concentrations and temperature gradient are particularly evident. In the latter instance, the flame zone model predicts a higher value which corresponds to an increase in the conductive heat transfer to the wall. This is partially balanced by a decrease in heat flux to the wall by diffusion as revealed by closer inspection of the concentration gradients at the wall. The net result is a slight increase in the total heat transfer to the wall, q, defined by (30) over the value obtained by the flame sheet analysis. This is shown in Fig. 6.

It is interesting to note that despite the considerable differences predicted by the two models in the detailed structure of the boundary layer, a gross effect such as the heat transfer q remains essentially unaffected.

The results obtained by use of the flame zone model have not been compared with the model proposed by Cohen [3] since for the conditions used in the present calculations the static temperatures within the boundary are too low for the concept of a dissociation temperature to be applicable.

CONCLUDING REMARKS

In this report a model for combustion within a boundary layer has been described and applied to the case of hydrogen or hydrogen–oxygen mixtures injected through a porous surface. The model which is termed the flame zone model utilizes the concept of a critical temperature to define regions of frozen flow, i.e. no reaction and regions of chemical equilibrium. The latter regions correspond to the flame zones.

The analysis corresponding to this model has been carried out for laminar flows of the similar type with the usual simplifying assumptions with respect to transport and thermodynamic properties, i.e. Prandtl and Lewis numbers equal to unity and the $\rho\mu$ product equal to constant. The hydrogen–oxygen–air system has been considered with nitrogen treated as an inert diluent.

Numerical examples indicative of wind tunnel and flight conditions were carried out to examine the features of hydrogen burning within the boundary layer according to the proposed model. The heat transfer to the porous surface is considered in detail. There are shown typical temperature and concentration profiles indicating the effects of coolant composition, surface temperature, free stream Mach number and free stream stagnation temperature. The distinctions between the proposed flame zone and the usually treated flame sheet model of chemical reaction are emphasized.

REFERENCES

1. J. A. Fay and F. R. Riddell, Theory of stagnation point heat transfer in dissociated air, *J. Aero. Sci.* **25**, 2, 73–85 (1958).
2. M. R. Dennison and D. A. Dooley, Combustion in the laminar boundary layer of chemically active subliming surfaces, *J. Aero. Sci.* **25**, 4, 271–272 (1958).
3. C. B. Cohen, R. Bromberg and R. P. Lipkis, Boundary layers with chemical reactions due to mass addition, *Jet Propulsion*, **28**, 10, 659–668 (1958).
4. R. Bromberg and R. P. Lipkis, Heat transfer in boundary layers with chemical reactions due to mass addition, *Jet Propulsion*, **28**, 10, 668–674 (1958).
5. J. P. Hartnett and E. R. G. Eckert, Mass transfer cooling with combustion in a laminar boundary layer. *Proceedings of the Heat Transfer and Fluid Mechanics Institute*, Stanford University Press, pp. 65–68, June (1958).
6. L. Lees, Convective heat transfer with mass addition and chemical reactions. *Combustion and Propulsion*, Third AGARD Colloquium, Palermo, Pergamon Press, New York, pp. 451–498 (1958).
7. A. A. Hayday, Mass transfer cooling in a steady laminar boundary layer near the stagnation point. *1959 Heat Transfer and Fluid Mechanics Institute*, Stanford University Press (1959).
8. A. Q. Eschenroeder, Combustion in the boundary layer on a porous surface, *J. Aero. Sci.* **27**, 12, 901–906. (1960).
9. J. A. Moore and M. Zlotnick, *Combustion of Carbon in an Air Stream*, AVCO Corporation, Research and Advanced Development Division, Technical Report RAD TR-T-60-32, December (1960).
10. E. R G. Eckert, P. J. Schneider, A. A. Hayday and R. M. Larson, Mass transfer cooling af a laminar boundary layer by injection of a light-weight foreign gas, *Jet Propulsion*, **28**, 1, 34–39 (1958).
11. H. W. Emmons and D. C. Leigh, Tabulation of the Blasius function with blowing and suction. Aeronautical Research Council Report No. 15, 996, June (1953).
12. J. A. Nicholls, Stabilization of gaseous detonation waves with emphasis on the ignition delay zone. Thesis for the degree of Doctor of Philosophy, University of Michigan, 1960 (available through University Microfilms, Inc., Ann Arbor, Michigan).
13. R. W. Duff, Calculation of reaction profiles behind steady state shock waves—I. Application to detonation waves, *J. Chem. Phys.* **28**, 6, 1193 (1958).

14. P. A. LIBBY, H. PERGAMENT and M. H. BLOOM, A theoretical investigation of hydrogen–air reactions. Part I—Behavior with elaborate chemistry. General Applied Science Laboratories, Inc., Technical Report No. 250, AFOSR 1378, August (1961).
15. S. S. PENNER, *Chemistry Problems in Jet Propulsion*. Pergamon Press, New York (1957).

APPENDIX A

The energy balance at blowoff

It is of interest to consider the dependence of the coolant temperature corresponding to an energy balance on the injection rate as the blowoff rate is approached.

Consider (52); at blowoff $c_f/c_{f_o} \to 0$, so that $q/q_o \to 0$. Hence, from (34), $h_c \to h_w$. Furthermore, as $-f_w$ approaches the blowoff value from (27) it may be seen that $\xi \to \infty$. Taking the limit as $\xi \to \infty$ in (26), (28), (29), and (44) yields

$$\tilde{Y}_{1w} \to \frac{\phi}{1+\phi}, \qquad \tilde{Y}_{2w} \to \frac{1}{1+\phi} \tag{A-1}$$

and

$$Y_{4w} \to 0, \qquad Y_{1w} \to \frac{\phi}{1+\phi}. \tag{A-2}$$

Hence,

$$Y_{3w} \equiv \frac{2W_3}{W_1}(\tilde{Y}_{1w} - \tilde{Y}_1) \to 0 \tag{A-3}$$

$$Y_{2w} \equiv \left(\tilde{Y}_{2w} - \frac{W_2}{W_3} Y_{3w}\right) \to \frac{1}{1+\phi}. \tag{A-4}$$

Referring to (18) it follows that (A-1)–(A-4) imply

$$\begin{aligned} Y_{1w} &= Y_{1c} \\ Y_{2w} &= Y_{2c} \\ Y_{3w} &= Y_{4w} = 0 \end{aligned} \tag{A-5}$$

so that the composition at the wall is identical to that in the coolant chamber; hence, $T_c \to T_w$ for $-f_w$ approaching the blowoff value.

Résumé—On propose un modèle de réaction chimique dans une couche limite laminaire basé sur la conception d'une température critique séparant les régions de l'écoulement gelé et de l'écoulement en équilibre. Le modèle, qui rappelle celui de la zone de flamme, est appliqué à l'injection, à travers une surface poreuse, dans une couche limite laminaire de mélanges H–O, les conditions extérieures dans l'air étant uniformes. On montre que le modèle est moins restrictif que le modèle de flamme fréquemment utilisé, auquel il se réduit dans des cas particuliers en faisant une approximation simplificatrice en ce qui concerne la condition d'équilibre. On présente les résultats de plusieurs exemples numériques relatifs à une soufflerie hypersonique et aux conditions de vol hypersonique.

Zusammenfassung—Für chemische Reaktionen in der Grenzschicht wird ein Modell vorgeschlagen, das eine kritische Temperatur als Unterscheidungsmerkmal zwischen den Bereichen der eingefrorenen und der Gleichgewichtsströmung definiert. Das Modell wird Flammzonenmodell genannt. Das Einblasen von Wasserstoff-Sauerstoff-Gemischen in Luft durch eine poröse Oberfläche in die laminare Grenzschicht mit gleichmässigen äusseren Bedingungen wird damit erläutert. Es zeigt sich, dass dieses Modell weniger Einschränkungen erfordert als das häufig verwendete Flammenstreifenmodell; auf letzteres ist es in Sonderfällen und mit einer vereinfachenden Annahme über die Gleichgewichtsbedingung zurückführbar. Die Ergebnisse verschiedener Beispiele, die hypersonischen Windkanal- und Flugbedingungen entsprechen, sind angegeben.

Аннотация—Предложена модель химической реакции в ламинарном пограничном слое, использующая критическую температуру для разграничения замороженного и равновесного потока. Эта модель называется моделью зоны пламени и применяется к процессу вдува водородно-кислородных смесей через пористую поверхность в ламинарный пограничный слой воздуха при однородных внешних условиях. Показано, что эта модель менее ограничена, чем обычная модель слоя пламени, применимая в частных случаях с использованием упрощающего допущения равновесных условий. Приводятся численные примеры для условий сверхзвуковой аэродинамической трубы и сверхзвукового полёта.